



LAWRENCE
LIVERMORE
NATIONAL
LABORATORY

Laser Damage Growth in Fused Silica with Simultaneous 351 nm and 1053 nm irradiation

M. A. Norton, A. V. Carr, C. W. Carr, E. E. Donohue, M.
D. Feit, W. G. Hollingsworth, Z. Liao, R. A. Negres, A.
M. Rubenchik, P. J. Wegner

October 31, 2008

Boulder Damage Symposium
Boulder, CO, United States
September 22, 2008 through September 24, 2008

Disclaimer

This document was prepared as an account of work sponsored by an agency of the United States government. Neither the United States government nor Lawrence Livermore National Security, LLC, nor any of their employees makes any warranty, expressed or implied, or assumes any legal liability or responsibility for the accuracy, completeness, or usefulness of any information, apparatus, product, or process disclosed, or represents that its use would not infringe privately owned rights. Reference herein to any specific commercial product, process, or service by trade name, trademark, manufacturer, or otherwise does not necessarily constitute or imply its endorsement, recommendation, or favoring by the United States government or Lawrence Livermore National Security, LLC. The views and opinions of authors expressed herein do not necessarily state or reflect those of the United States government or Lawrence Livermore National Security, LLC, and shall not be used for advertising or product endorsement purposes.

Laser Damage Growth in Fused Silica with Simultaneous 351 nm and 1053 nm irradiation

Mary A. Norton, Adra V. Carr, C. Wren Carr, Eugene E. Donohue, Michael D. Feit, William G. Hollingsworth, Zhi Liao, Raluca A. Negres, Alexander M. Rubenchik, P. J. Wegner

Lawrence Livermore National Laboratory, M/S L592, PO Box 5508, Livermore, CA 94551

ABSTRACT

Laser-induced growth of optical damage often determines the useful lifetime of an optic in a high power laser system. We have extended our previous work on growth of laser damage in fused silica with simultaneous 351 nm and 1053 nm laser irradiation by measuring the threshold for growth with various ratios of 351 nm and 1053 nm fluence. Previously we reported that when growth occurs, the growth rate is determined by the total fluence. We now find that the threshold for growth is dependent on both the magnitude of the 351 nm fluence as well as the ratio of the 351 nm fluence to the 1053 nm fluence. Furthermore, the data suggests that under certain conditions the 1053 nm fluence does not contribute to the growth.

Keywords: Laser damage, UV laser damage, laser damage growth, UV fused silica.

1. INTRODUCTION

The lifetime of optics used in laser applications is limited both by laser initiated damage and by the subsequent growth of the laser initiated damage. This work is concerned with only the growth of damage. The National Ignition Facility (NIF) is a 1.053 μm wavelength (1ω) laser frequency converted to 351 nm (3ω) for irradiation of the target. Frequency conversion of the highly shaped pulses required for ignition experiments is typically only 55% to 65% efficient, with the majority of the residual light at the drive frequency (1ω) thus the growth of laser-initiated damage in the downstream fused silica transport optics under the simultaneous irradiation of both 1ω and 3ω wavelengths is of interest in predicting the lifetime and operational cost of these optics.

Previous work has measured the growth rate of laser-induced damage in UV grade fused silica exposed to 3ω alone¹, to 1ω alone² and with combined 1ω and 3ω light when the 3ω fluence was near or greater than the 3ω -only growth threshold³. This work extends the measurements of growth rates for simultaneous 1ω and 3ω irradiation to include the case where the 3ω component is less than the 3ω -only growth threshold. A significant finding in this work is that the growth rate of the lateral size is set by the sum of the 3ω fluence and the fraction of the 1ω fluence that arrives after the growth is initiated.

2. BACKGROUND

To make measurements of laser damage growth that are relevant to large beam areas as will be found on the NIF, it is necessary to use a beam with an area large relative to the initial damage size. The growth of laser damage on the exit surface of fused silica has been measured with a beam area $\sim 5\times$ the final area of the grown damage site. The growth in lateral diameter is exponential with shot number over more than one order of magnitude in diameter, and is described by:

$$d = d_0 e^{\alpha N}$$

where d is the lateral diameter, N is the shot number and α is the growth coefficient.

Our previous measurements of the growth coefficient are plotted versus total fluence for both simultaneous 1ω and 3ω illumination and for 3ω -only illumination as shown in Figure 1. In the following, the 3ω fluence and the 1ω fluence are referred to as $\phi_{3\omega}$ and $\phi_{1\omega}$ respectively. A linear fit to the $\phi_{3\omega}$ -only data shows a threshold effect where the required fluence for growth $\phi_{3\omega}$ -only is $\phi_{3\omega}(\text{TH}) = 5 \text{ J/cm}^2$. The data taken with the two simultaneous wavelengths is found to agree reasonably well with the $\phi_{3\omega}$ -only fit when plotted versus the total sum fluence. The sum-fluence data in Figure 1 was obtained for cases where $\phi_{3\omega} > \phi_{3\omega}(\text{TH})$. For operation under conditions with low conversion efficiency there are likely to be

situations where the 3ω fluence will be less than the 3ω -only growth threshold. This is the condition that is emphasized in the current work.

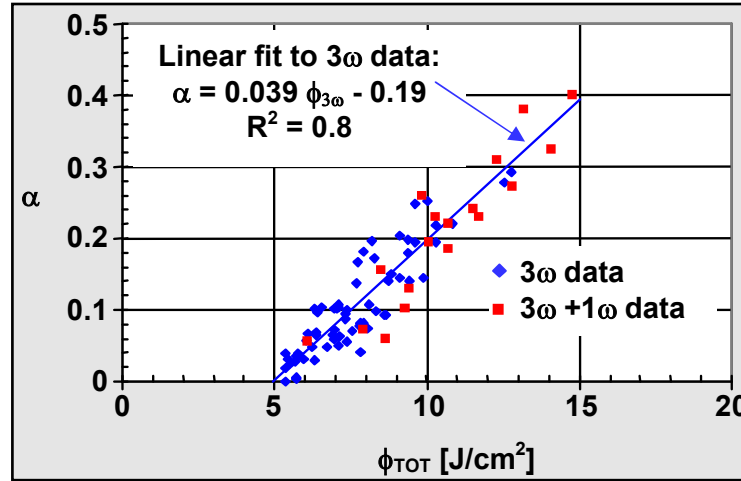


Figure 1. Damage growth coefficients for 3ω -only and simultaneous 3ω and 1ω illumination with $\phi_{3\omega} > 5 \text{ J/cm}^2$.

3. EXPERIMENTAL DETAILS

The growth measurements are made with the SLAB laser system⁴, a Nd: glass zig-zag slab amplifier, with SBS phase conjugation. It outputs a 351 nm beam of 8 J, with a 10 to 12 nsec FWHM near Gaussian pulse shape at a rate of 0.5-Hz. The repetition rate is limited by the data collection rate as the laser system has the capability of 4 Hz operation. In practice the 1-micron laser output beam is image relayed to a type I/type II KD*P tripler frequency converter. All three colors are then passed through a vacuum relay with a magnification of two before reflecting from two dichroic mirrors where the unconverted green light is dumped and the UV and infrared are sent back through this same relay. The output of this relay is then passed through two additional vacuum relays, one for the UV and one for the infrared, where each wavelength is spatially filtered before it is recombined and transported to the sample chamber. A schematic of the set-up showing the path from the 1ω and 3ω beam-combining dichroic through the sample as well as the diagnostics used for these tests is shown in Figure 2. The test sample is located in an image relay plane of the laser and the beam sizes on the part are nominally 5 mm x 5 mm. The contrast ratio of the beams in the 1mm region surrounding the damage site is typically ~10%.

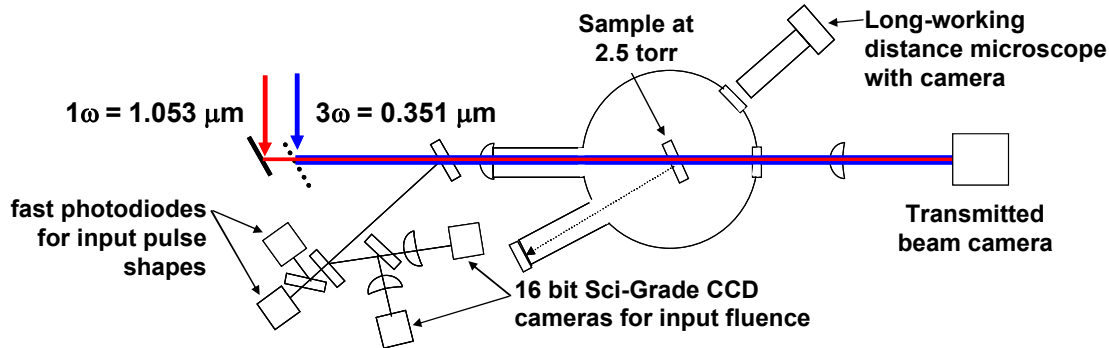


Figure 2. Experimental layout for growth experiments.

The sample is housed in a stainless steel vacuum chamber which is located in a class 100 clean room where samples are handled during loading. These tests were conducted in air at 2.5 torr. Laser beam diagnostics for both wavelengths include measurement of the temporal pulse shape, energy, and input & output beam near field intensity profiles. Diagnostics to measure the growth include a white light illuminated, long working distance microscope and CCD camera and scientific grade CCD cameras imaging the site with the transmitted light. The main diagnostics for the growth measurements are 16-bit scientific-grade CCD cameras that sample the input beams. They are calibrated both for energy and for magnification and are used to set the fluence for each wavelength on the sample. In practice the camera viewing the beam transmitted through the

sample is used to locate the starting damage and the input cameras are used to set the local fluence in a 1-mm patch surrounding the site. The lateral growth of the damage site can be measured either from the transmitted camera or from the microscope.

The samples are 2-inch round fused silica 1-cm thick, UV grade Corning 7980 and were super polished by SESO. Approximately half of the damage sites studied were laser-initiated with a small-beam, frequency-tripled ND-YAG laser operating at 351 nm with a single shot at fluence levels near 40 J/cm^2 with an 8 nsec FWHM Gaussian pulse. This high initiating fluence was chosen to produce approximately repeatable damage spots in both size and morphology, typically composed of a cluster of pits (Figure 3a). In addition, about half of the sites studied were mechanically indented with a 2 N Vickers indenter. These mechanically initiated sites were subsequently grown with 3ω illumination, to achieve a lateral size in the range of $50\text{-}80 \text{ }\mu\text{m}$ in order to insure that these starting morphologies were similar (Figure 3b). All samples were oriented with the damage sites on the exit surface for all growth measurements.

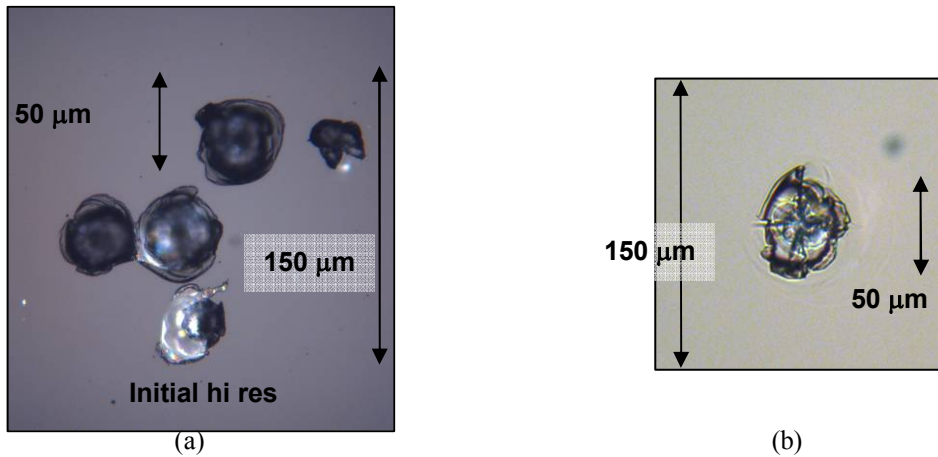


Figure 3. Micrographs of typical starting morphologies for a) a laser initiated site and b) a mechanically initiated site grown with 3 shots at 9 J/cm^2 , 3ω .

4. EXPERIMENT RESULTS

4.1 Non-exponential growth behavior

Approximately 60 new damage sites were studied in this test series; about half of the sites were laser initiated and the other half were mechanically initiated with a 2 N Vickers indent tool. Various shot protocols were followed on these sites yielding $1\omega/3\omega$ fluence pairs for which no changes in size or morphology were observed, fluence pairs for which changes occurred within 1 or 2 laser shots which then remained stable for tens of additional shots, and finally fluence pairs for which changes continued with each subsequent shot. It is this last condition which follows an exponential increase in diameter with shot number.

Many of the sites studied in these tests were illuminated under simultaneous wavelength conditions which produced no exponential growth. Under these conditions there was either no physical change visible in the online microscope or a change was observed on one or a few shots followed by at least 15 to 30 shots during which no further changes were observed. This behavior is illustrated in Figure 4 for a laser initiated site that was tested with 8 combinations of fluence before exponential growth was observed. This figure plots both the 3ω fluence and 1ω fluence vs. shot number along with low resolution micrographs showing the discrete changes observed. For the entire sequence of 364 shots the 1ω fluence was held nominally at 4 J/cm^2 and as can be seen in the plot the shot to shot variation in the 1ω fluence was high for the first 100 shots. For each combination of simultaneous wavelengths the site was shot 50 times. The high resolution off-line initial micrograph of the site in Figure 4a shows that this laser initiated site consisted of 2 isolated pits; a $30 \text{ }\mu\text{m}$ pit and a $50 \text{ }\mu\text{m}$ pit. The corresponding initial low resolution on-line microscope image is shown in Figure 4b. The site showed no changes occurring (within the limit of the on-line microscope resolution) for first 200 shots. When the 3ω fluence was increased to 4 J/cm^2 two discrete changes were observed; the largest change was a 30% diameter increase as seen in Figure 4c. The following 27 shots

at the same condition produced no further change. The next sequence increased the 3ω fluence to 5 J/cm^2 and after 44 shots a diameter increase of 60% was observed in the larger pit as seen in Figure 4d. The next sequence increased the 3ω fluence to 6 J/cm^2 and after 21 shots a diameter increase of 170% was observed in the smaller pit with no further increases in either pit for the next 29 shots as seen in Figure 4e. The next sequence increased the 3ω fluence to 8 J/cm^2 which led to changes producing exponential growth and will be discussed in the next section.

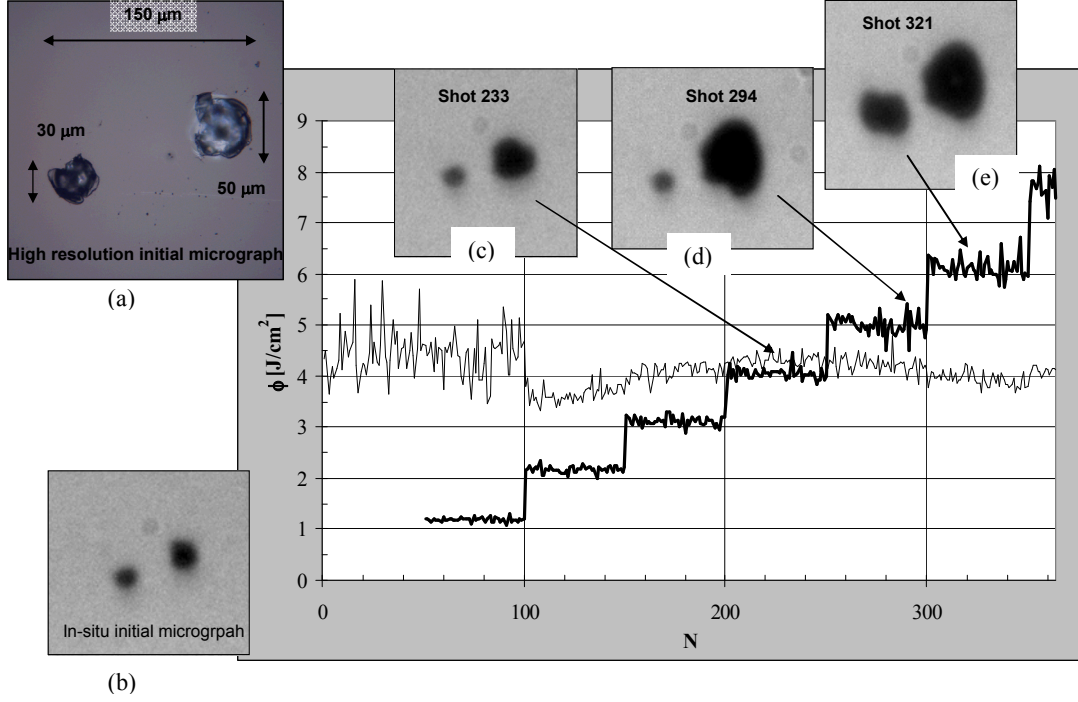


Figure 4. Example of morphology changes observed at fluences below those required for exponential growth.

4.2 Exponential growth data

For those damage sites which were illuminated under conditions producing sequential growth, the diameter versus shot number was plotted and the data fit to an exponential form from which the growth coefficient was determined. Hence, in these cases, the exponential growth coefficient is explicitly a function of both fluences: $\alpha(\phi_{3\omega}, \phi_{1\omega})$. For the site followed in Figure 4 these conditions were met at $\phi_{3\omega} = 7.8 \text{ J/cm}^2$ and $\phi_{1\omega} = 4.3 \text{ J/cm}^2$. A sequence of 14 shots produced exponential growth in diameter and both selected micrographs and the shot fluence plot for these shots are shown in Figure 5. As seen in these images it is the smaller pit that begins the growth sequence. The plots of the diameter vs. shot number along with the exponential fit to this data are also shown in Figure 5.

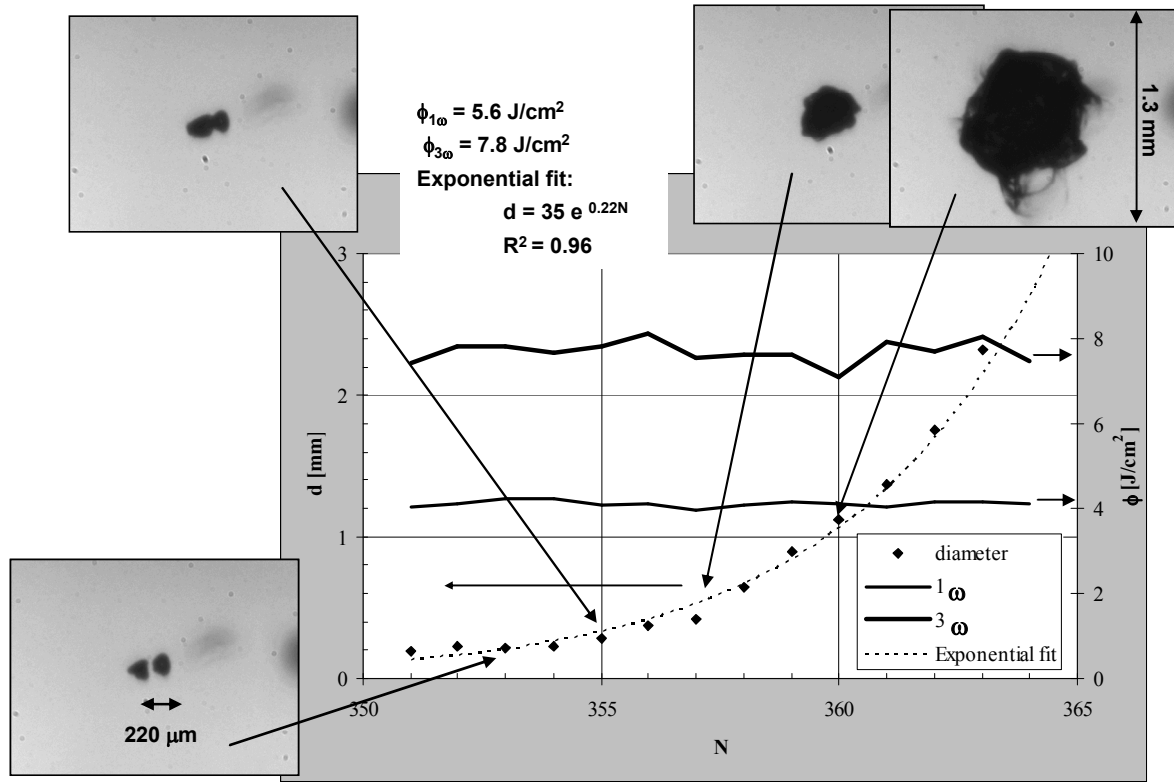


Figure 5. Example of typical exponential growth shot sequence.

Figure 6 plots the simultaneous multi-wavelength growth data versus the total fluence, $\phi_{\text{TOT}} = \phi_{3\omega} + \phi_{1\omega}$, for various amounts of the 3ω component fluence. From this plot, it is seen that the departure of the simultaneous growth coefficients from the 3ω -only linear fit increases as the 3ω component decreases. Hence, $\alpha(\phi_{3\omega}, \phi_{1\omega})$ cannot be written simply as $\alpha(\phi_{\text{TOT}})$.

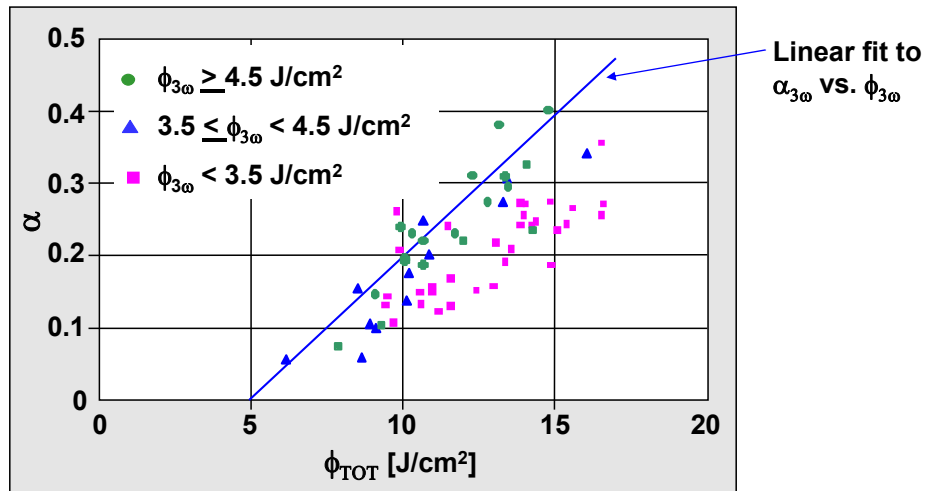


Figure 6. New data set showing simultaneous multi-wavelength data parameterized by magnitude of the 3ω component.

An important consideration for the simultaneous wavelength growth data is the relative temporal delivery of the two wavelengths. In these tests, it is the unconverted 1ω fluence that is recombined with the converted light and is then delivered to the test site. This means that for all temporal shapes, except those that are flat in time, the converted wavelength will have a shorter pulse shape than will the fundamental and in fact depending on the conversion efficiency the two wavelengths may show very different structure and width. For these tests, the conversion efficiency is typically around 40% to 50% and the resulting waveforms that are typical of those when the 3ω component is near 3 J/cm^2 are shown in Figure 7.

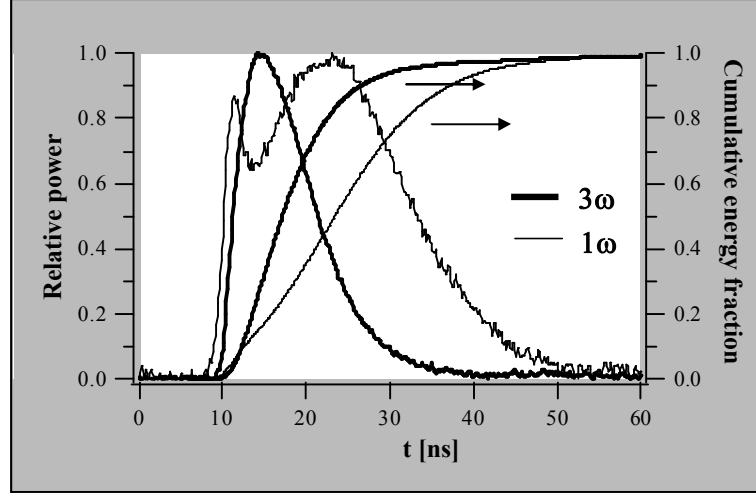


Figure 7. Plots of instantaneous power and cumulative energy fraction for both wavelengths.

5. DISCUSSION

5.1 Contribution of the 1ω component to exponential growth

The following scenario can help to understand the experimental results. The damage spot is comprised of some thickness of modified material. The light propagating from the input surface can be partially absorbed by the modified material, initiating breakdown and a plasma layer inside the material. The threshold for the plasma generation is much lower for 3ω light. When a plasma is produced, it effectively absorbs both wavelengths. The plasma pressure which initiates the cracking and modification of the material is determined by the total absorbed energy. Hence, at high enough fluences the growth is determined by the total fluence. For modest levels of blue light the plasma forms only near the peak of 3ω pulse and all 1ω energy arriving before this moment does not participate in the damage growth.

The time dependence of irradiance of both wavelengths for the case of $\phi_{3\omega}=3 \text{ J/cm}^2$ is shown in Figure 7. If we postulate that the long wavelength component makes no contribution to the growth before the short wavelength component starts the growth, then the simultaneous wavelength data is brought into close agreement with the 3ω growth coefficient dependence on fluence. To illustrate this point, we assume that the 1ω energy that arrives before the 3ω reaches approximately its peak irradiance does not couple into the growth. For the case shown in Figure 7 this means that $\sim 30\%$ of the 1ω component would not be added to the 3ω fluence when calculating the total fluence. This is shown in Figure 8a where we plot the growth coefficient for 3ω only, $\alpha(\phi_{3\omega}, \phi_{1\omega}=0)$ (straight line) along with the simultaneous wavelength data for the case of the $\phi_{3\omega} < 3.5 \text{ J/cm}^2$, $\alpha(\phi_{3\omega} < 3.5 \text{ J/cm}^2, \phi_{1\omega})$. Here, we write the growth coefficient as a function of both the total fluence and the total fluence using only 70% of the 1ω component fluence. Clearly, the fit with the 3ω -only data is much better when $\phi_{\text{TOT}} = \phi_{3\omega} + 0.7\phi_{1\omega}$.

Similar considerations applied to the other two 3ω fluence bins have been applied to the temporal waveforms and the results are plotted in Figure 8b where the sum fluence is the sum of the entire 3ω fluence plus a fraction, β , of the 1ω fluence. We find that for 3ω fluence between 3.5 and 4.5 J/cm^2 , 20% of the 1ω component is ineffective in contributing to growth. For the case of $3\omega > 4.5 \text{ J/cm}^2$ we find that only 10% of the 1ω component does not contribute to the growth.

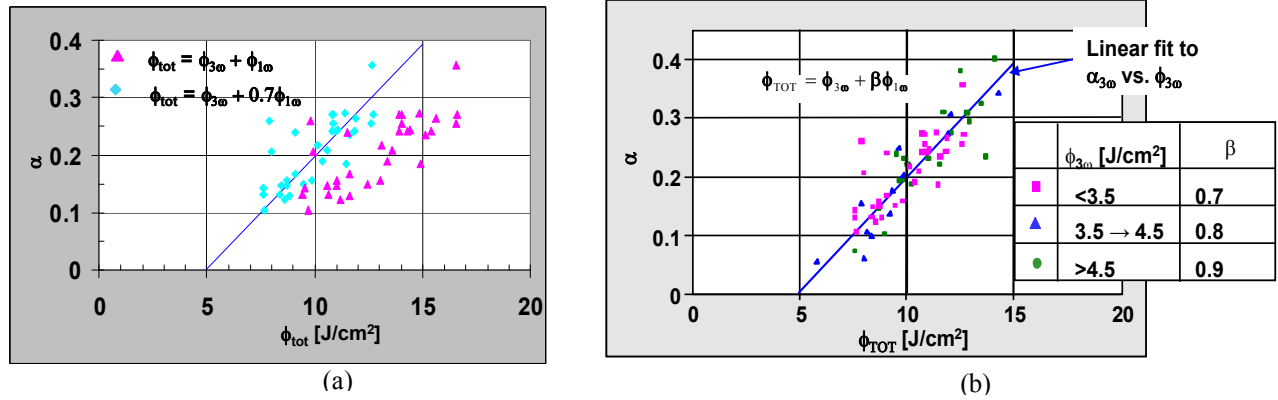


Figure 8. Growth coefficients for simultaneous wavelength exponential growth as a function of modified total fluence.

5.2 Two types of growth behavior

Two distinct growth behaviors have been observed during the course of these tests. The first region is characterized by the site experiencing sporadic changes in morphology. This behavior may be a discrete change occurring in a single shot or it may be changes occurring over as many as 3 shots. It is not typically followed with exponential growth at the same set of simultaneous fluence conditions. The second growth behavior is characterized by changes in morphology that evolve into exponential growth within a few shots and continues to do so under the same set of fluence conditions.

The observed results are consistent with the qualitative picture presented in the discussion of the previous section. For low enough fluence the threshold for plasma formation can be sensitive to the specific non-reproducible morphology of the damage spot. For the same fluence the spots with different morphologies can grow or not grow. If the plasma is produced only in some parts of the damaged spot, the following material modification can arrest the growth by subsequent pulses.

5.3 Probability of growth

Since we currently do not have the tools available to reliably predict at what fluence a damage site will be induced to grow exponentially, we find it expedient to introduce the probability of growth for a damage site under a given set of conditions. All of the data has been grouped into 3 fluence bins for the 3ω fluence and the probability that exponential growth was observed is plotted vs. the 1ω fluence component. This data is shown in Figure 9. The data set at $\phi_{3\omega}=3$ J/cm² is the most extensive, but even so, it is sparse; for this data set we have drawn a straight line to schematically illustrate the trend of the dependence. This straight line has then been shifted along the x axis and a qualitative agreement with the remaining two data sets is seen. This result suggests that for $\phi_{3\omega} < \phi_{3\omega}(\text{TH})$, the probability for exponential growth increases linearly with 1ω fluence, and is strongly affected by how far the 3ω fluence is below $\phi_{3\omega}(\text{TH})$ – the closer $\phi_{3\omega}$ is to $\phi_{3\omega}(\text{TH})$, the higher the probability of exponential growth. When $\phi_{3\omega}$ is well above $\phi_{3\omega}(\text{TH})$, the probability for exponential growth is essentially one, and the growth rate coefficient can be written as a function of the sum fluence, $\phi_{3\omega} + \phi_{1\omega}$.

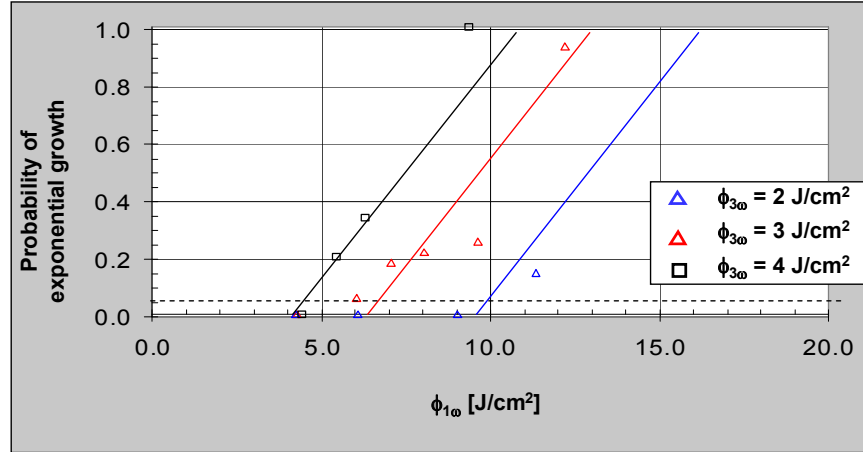


Figure 9. Probability of observing exponential growth.

6. CONCLUSIONS

We have established that when simultaneous multi-wavelength laser damage growth with 3ω and 1ω wavelengths produces exponential growth the exponential growth coefficient is determined by both fluence components. The dependence of the growth coefficient on fluence follows the 3ω only fluence dependence when the total fluence is calculated as the sum of the two components where the long wavelength contributes only after the peak of the 3ω intensity is reached. This view is consistent with the idea that the 3ω component initiates a plasma and after this occurs the entire remaining 1ω component couples into the growth.

Though this interpretation is valid for exponential growth when it occurs, we find that there is a behavior where no growth or sporadic discrete changes occur even when the total modified fluence exceeds the growth threshold. This behavior is most conveniently described by considering the probability of growth. This interpretation can be used to predict the fluence conditions under which there is less than an acceptable risk of damage growth. Future work along these lines will help in the identification of the precursors for growth.

ACKNOWLEDGEMENTS

This work was performed under the auspices of the U. S. Department of Energy by Lawrence Livermore National Laboratory under Contract DE-AC52-07NA27344.

1. M. A. Norton, L. W. Hrubesh, Z. Wu, E. E. Donohue, M. D. Feit, M. R. Kozlowski, D. Milam, K. P. Neeb, W. A. Molander, A. M. Rubenchik, W. D. Sell, and P. J. Wegner, "Growth of laser-initiated damage in fused silica at 351 nm", *Proc. SPIE* 4347, 468, 2000.
2. M. A. Norton, E. E. Donohue, W. G. Hollingsworth, M. D. Feit, A. M. Rubenchik, and R. P. Hackel, "Growth of laser-initiated damage in fused silica at 1053 nm", *Proc. SPIE* 5647, 197, 2004.
3. M. A. Norton, E. E. Donohue, M. D. Feit, R. P. Hackel, W. G. Hollingsworth, A. M. Rubenchik, and M. L. Spaeth, "Growth of laser damage in fused SiO₂ under multiple wavelength irradiation", *Proc. SPIE* 5991, 08, 2005.
4. C. B. Dane, L. E. Zapata, W. A. Neuman, M. A. Norton, and L. A. Hackel, "Design and operation of a 150 W near diffraction-limited laser amplifier with SBS wavefront correction," *IEEE J. Quantum Electronics*, **31**, pp. 148-163, 1995.